

CHEMISTRY

A European Journal

A Journal of



Accepted Article

Title: Surface-active fluorinated quantum dots for enhanced cellular uptake

Authors: Pablo G. Argudo, Mónica Carril, María T. Martín-Romero, Juan J. Giner-Casares, and Carolina Carrillo-Carrión

This manuscript has been accepted after peer review and appears as an Accepted Article online prior to editing, proofing, and formal publication of the final Version of Record (VoR). This work is currently citable by using the Digital Object Identifier (DOI) given below. The VoR will be published online in Early View as soon as possible and may be different to this Accepted Article as a result of editing. Readers should obtain the VoR from the journal website shown below when it is published to ensure accuracy of information. The authors are responsible for the content of this Accepted Article.

To be cited as: *Chem. Eur. J.* 10.1002/chem.201804704

Link to VoR: <http://dx.doi.org/10.1002/chem.201804704>

Supported by
ACES

WILEY-VCH

Surface-active fluorinated quantum dots for enhanced cellular uptake

Pablo G. Argudo,^a Mónica Carril,^{b,c} María T. Martín-Romero,^a Juan J. Giner-Casares^{*a} and Carolina Carrillo-Carrión^{*d,e}

Abstract: Fluorescent nanoparticles such as quantum dots have exciting possibilities for biomedical applications, mainly sensing and bioimaging. However, the inefficient cell uptake of some nanoparticles remains as a frontier for their application in clinical practice. Herein we explore the effect of modifying the quantum dot's surface with fluorinated ligands for increasing their surface activity and hence enhancing their cellular uptake.

Much effort is being directed towards understanding the cellular uptake of nanoparticles (NPs) in order to design novel nanostructures with improved bioperformance, and consequently having a higher efficiency for biomedical uses such as in bioimaging, intracellular sensing, and drug delivery, among others.¹⁻⁴ In this direction, advances in functionalization strategies to optimize cellular uptake and trafficking, and methodologies for revealing the underlying parameters controlling the nano-cellular interactions are of utmost importance.^{5,6} The first major barrier against the influx of exogenous material inside a cell is the impermeable phospholipid bilayer of the cellular membrane, which is often unpredictable. While the effects of physicochemical properties of NPs such as size, shape, stiffness, charge, and surface chemistry have been widely studied,⁷⁻¹² the role of the surface hydrophobicity/hydrophilicity in the cellular uptake of NPs, which is still not well understood, is garnering increasing attention lately.¹³⁻¹⁶ On the one hand, it is generally accepted that hydrophobic and interfacial forces play important roles in the interaction between NPs and cellular membranes. Molecular dynamic simulations clearly showed that hydrophobic NPs are thermodynamically stable around the middle of the hydrophobic core of a cell membrane, whereas a semihydrophilic NP is only found to adsorb into the membrane.^{14,15} Recently, Shastri et al. described the preparation of polymeric NPs with increasing hydrophobicity by copolymerization with lipid components of cell

membranes, and found an increased cellular uptake of the most hydrophobic NPs.¹⁶ Similarly, Sung et al., based on both experimental evidence and molecular dynamic simulations, reported that the cellular uptake of hydrophobically modified chitosan was enhanced with increasing their hydrophobic character.¹⁷ On the other hand, the impact of fluorine on the interaction of bioactive molecules with cells is profound, due to mainly its high hydrophobicity. It is indeed not a coincidence that fluorine is present in around 20% of current pharmaceutical compounds, and much of the optimization process in drug development is focused on the modification of active compounds with fluorine atoms.¹⁸⁻²⁰

In spite of this knowledge, the modification of NPs with fluorinated ligands for increasing their hydrophobicity as well as for exploiting the effect of fluorine on the interaction with cells is poorly investigated, and little is known about the cellular uptake of fluorinated NPs.²¹

Herein, we report the fluorination of NPs as a straightforward strategy to modulate their interactions with cells and subsequent cellular uptake. To give insight into the mechanism underlying the differential cellular uptake of fluorinated NPs, the interaction of these NPs with a cell membrane model is studied. In particular we focus on fluorescent quantum dots (QDs) owing to its superior properties as bioimaging probes in comparison to conventional organic fluorophores.²²⁻²⁴

In this work fluorinated QDs (in the following referred to as QD_F) were prepared by ligand-exchange of trioctylphosphine oxide (TOPO)-capped ZnCdS/ZnS QDs (in the following referred to as QD_TOPO) with the fluorinated ligand HS-C₁₁-(EG)₄-O-C(CF₃)₃ (Fig. 1A, see details in ESI). The use of this ligand containing a perfluoro-tert-butyl group allows for the introduction of a high amount of fluorine atoms on the outer surface of the QDs, whereas the ethylene glycol units in the linker enhance the solubility. The as-prepared QD_TOPO and QD_F NPs presented an inorganic core/shell diameter of (7.0 ± 0.5) nm as determined by transmission electron microscopy (TEM, Fig. S1), and maximum emission fluorescence at ca. 435 nm under excitation at 350 nm (Fig. S2). The emission spectrum of the QD_F was slightly narrower than that of the QD_TOPO sample, which indicates a smaller particle size distribution. This may be as a result of the additional purification steps by centrifugation after the ligand exchange process, which could lead to the isolation of more homogeneous particles. In fact, the same observation was derived from the dynamic light scattering (DLS, Fig. S3) measurements, since the DLS spectrum of QD_F was also narrower and presented a smaller polydispersity index

[a] Institute of Fine Chemistry and Nanochemistry, Department of Physical Chemistry and Applied Thermodynamics, University of Córdoba, Campus Universitario de Rabanales, Edificio Marie Curie, E-14014 Córdoba, Spain. E-mail: jginer@uco.es

[b] Biofisika Institute (CSIC, UPV/EHU) and Department of Biochemistry and Molecular Biology, University of the Basque Country UPV/EHU, 48940 Leioa, Spain.

[c] Ikerbasque, Basque Foundation for Science, 48011 Bilbao, Spain

[d] CIC biomaGUNE, 20014 San Sebastian, Spain.

[e] Center for Research in Biological Chemistry and Molecular Materials (CiQUS), University of Santiago de Compostela, 15782 Santiago de Compostela, Spain. E-mail: carolina.carrillo@usc.es

Supporting information for this article is given via a link at the end of the document.

value. The hydrodynamic diameters, given as number distribution, were (10.5 ± 2.3) nm for QD_TOPO and (16.7 ± 1.7) nm for QD_F NPs. As it was expected the hydrodynamic size increased after the ligand exchange owing to the higher length of the fluorinated ligand in comparison to the TOPO. In both cases the low polydispersity index values demonstrated the good homogeneity of the NPs in terms of size. The presence of the fluorinated ligand on the QD surface after the functionalization, along with remaining TOPO, was confirmed by ^1H and ^{19}F NMR (Fig. S4). The non-fluorinated QD_TOPO were used as control as they are also hydrophobic but lack fluorine atoms. Interfacial tension measurements by using the pendant drop method revealed the hydrophobic character of both QDs, being the QD_F NPs more hydrophobic than QD_TOPO²⁵ (Fig. S5).

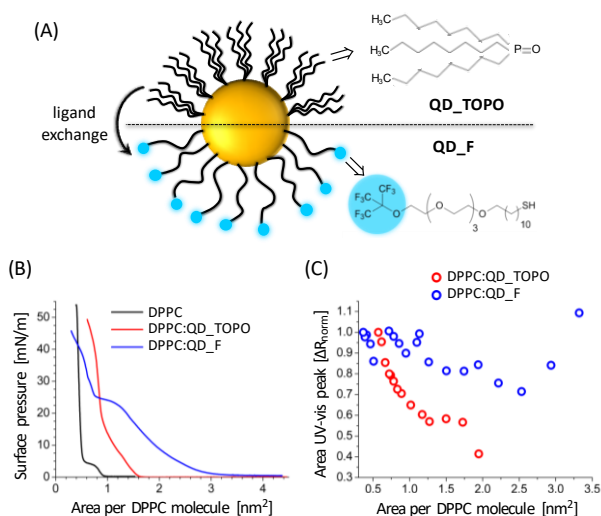


Figure 1. (A) Scheme of the two types of QDs studied, TOPO-capped QDs (QD_TOPO) and fluorinated QDs (QD_F). (B) Surface pressure-molecular area of a pure DPPC monolayer (black line), and DPPC monolayers with QD_TOPO (red line) or QD_F (blue line). (C) Value of integral of the UV-vis reflection spectra as a function of the area of the monolayer for DPPC:QD_TOPO (red circles) and DPPC:QD_F (blue circles).

In order to evaluate the influence of the ligand exchange process, and thus the change of the organic shell around, on the fluorescence emission efficiency of the QD, the quantum yield (QY) before and after the exchange was determined by the method outlined by Horiba, which is based on the comparative method work of Williams et al.²⁶ Details of the used procedure and calculations are given in the supporting information (cf. section II.3, Fig. S6). The determined QY values were 0.82 for QD_TOPO NPs and 0.77 for QD_F NPs, indicating that the exchange process did not affect significantly to the fluorescence efficiency.

To study first the potential interaction of both QDs types with cells, Langmuir monolayers of the phospholipid 1,2-dipalmitoyl-sn-glycero-3-phosphocholine (DPPC), which is a major constituent of the eukaryotic cell membrane, were used as model surface. This model allows mimicking the response of the cell membrane against the QDs.²⁷ For the formation of the

monolayer QDs and DPPC were cospread in a fixed optimized molar ratio, and thus the amount of QDs that might be at the DPPC interface is well-defined. A slight excess of DPPC molecules was included for the formation of a close-packed monolayer of QDs (Fig. S5).

Restricting the physical scenario to a simplified model allows us to discern the different behaviour of fluorinated and non-fluorinated NPs (QD_F versus QD_TOPO) exclusively as the result of the changes on the surface activity of the QDs.²⁸ The possibility of *in situ* studying the DPPC monolayer and the influence of the QDs at different values of molecular area per phospholipid molecule provides a detailed picture on the surface activity of the QDs. Taking into account that the inorganic core of the QD is the same in both cases the observed changes in the surface activity are due solely to the presence of different capping ligands on their surface, *i.e.* fluorinated and non-fluorinated ones.

Surface pressure-molecular area isotherms of the DPPC monolayers (Fig. 1B) offer information on the surface activity of the QDs and their interaction with the model DPPC surface.²⁹ The modification of the isotherm induced by the QD_F was significantly higher than by the QD_TOPO. The values of DPPC molecular area for the lift-off of surface pressure for pure water, QD_TOPO and QD_F were 0.9, 1.6, and 3.5 nm², respectively. The greater expansion of the isotherm recorded in presence of the QD_F indicates a higher occupancy of the DPPC interface by the QD_F, in contrast to the QD_TOPO. The shape of the isotherms was also significantly affected by the incorporation of QDs into the monolayer, pointing to a modification of the phase behaviour of the DPPC molecules in contact with the QD. In particular, the QDs exerted a fluidization of the DPPC monolayer by effectively interacting with the phospholipid molecules. Interestingly, such fluidization was greater for the QD_F when compared to the QD_TOPO, noted in a quantitative decrease of the compression modulus C_s^{-1} from 200 to 300 mN/m (liquid condensed and solid monolayer) for the pure DPPC and the DPPC:QD_TOPO monolayers to values from 0 to 50 mN/m (liquid expanded monolayer) for the DPPC:QD_F monolayer (Fig. S6). This effect arises from a significant interaction between the QD_F and the hydrophobic region of the DPPC monolayer. The available surface area per DPPC molecule was reduced by compression of the monolayer. The 2D clustering of QD_F with compression of the monolayer enhanced the hydrophobic interaction with the alkyl chains of the DPPC molecules. This interaction with the curved surface of the QD_F led to an effective removal of DPPC molecules from the monolayer to the QD_F surface, as observed in the area reduction at almost constant surface pressure of *ca.* 25 mN/m and the inter-crossing of the isotherm with the pure DPPC monolayer at *ca.* 41 mN/m (Fig. 1B). This enhancement in the hydrophobic interactions between the QD_F and the phospholipids is key for the superior cell uptake.

Taking advantage of the reflection band of QDs in the range of 250-500 nm,³⁰ the amount of either type of QD present at the DPPC interface along the isotherm could be monitored by *in situ* UV-vis reflection spectroscopy. For comparison the UV-vis reflection spectra obtained for both DPPC:QD_TOPO and DPPC:QD_F monolayers were integrated and normalized to the maximum value, *i.e.* the absorption at the most compressed state of the monolayer and therefore with the highest density of QDs at the interface. As presented in Fig. 1C, the QD_F were present in at least 80% of the maximum amount along the whole compression range, whereas the QD_TOPO were initially present only at 40% and their amount increased gradually with compression and only reached the maximum amount at a highly compressed state of the monolayer. The observed variation in intensity of the UV-vis reflection spectra with the decrease in molecular area of the DPPC was due to the enrichment of QD_F at the lipid/water interface. Such enrichment was connected to the increase of available DPPC molecules to interact with the QD_F, thus attracting and keeping a larger number of QD_F at the interface. The comparatively higher signal/noise ratio of the UV-vis reflection spectra of the QD_F with respect to QD_TOPO might arise from a larger aggregation at the air/liquid interface, see Figure S8. The aggregation of inorganic nanoparticles at the air/liquid interface led to micron-size domains of nanoparticles, resulting in a higher noise in the spectroscopic signal.³¹ Such domains were indeed visualized by microscopy, see below.

The change of the DPPC monolayer interfacial structure and organization induced by the QDs was monitored *in situ* by Brewster angle microscopy (BAM), allowing us to get insights into the micrometric domains. Interestingly, a contrast inversion took place for both QD types, in which the surrounding phase to the DPPC liquid condensed domains appeared brighter than the domains (Fig. 2 and S8). Images were taken at different values of the surface pressure, corresponding to different degrees of compression of the monolayer. These images clearly showed the lack of significant modification of the morphology of the DPPC monolayer in contact with QD_TOPO at a greater compression state of the DPPC monolayer (Fig. 2A), suggesting a comparatively modest occupancy of the interface. In contrast, the DPPC monolayer in contact with QD_F displayed a noticeable modification (Fig. 2B), in which the domains were disrupted and bright solid-like microstructures appeared. Such microstructures can be assigned to accumulation of the surface active QD_F into aggregates at the DPPC interfaces expected from the isotherm (see above), further confirming their greater surface activity.

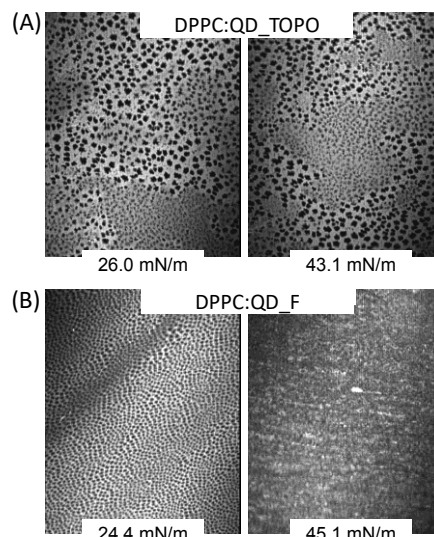


Figure 2. Brewster Angle Microscopy pictures of the DPPC monolayer in contact with (A) QD_TOPO, and (B) QD_F. Values of surface pressure for each picture are indicated in the insets. Width equals to 225 μm .

Once studied the interaction of different QDs with a cell membrane model, results clearly revealed a higher surface activity of QD_F resulting in an enhanced interaction at the phospholipid interface. Then, cellular uptake studies of the QDs were carried out in order to investigate if there is a correlation between the observations with the DPPC membrane model and the truly behavior in cells. To this end, HeLa cells were first incubated with both QD_F and QD_TOPO NPs at a concentration of 5 nM for 24 h. The cytotoxicity was evaluated obtaining that the cell viability decreased to around 80% as determined by MTT assay (Fig. 3A). However, such decrease may be attributed mainly to the presence of 0.5 % of DMSO which is needed for the proper dispersion of the hydrophobic NPs in the cell culture medium. In order to minimally affect the cell viability (*i.e.* maintaining viability $\geq 90\%$), the treatment of HeLa cells with NPs (5 nM) was reduced to 5 h, which demonstrated to be sufficient for sensitive uptake studies by confocal fluorescence microscopy (Fig. 4). It is important to note that the uptake studies were performed in serum-free medium for avoiding the potential adsorption of proteins around the QDs (*i.e.* formation of the so-called protein corona),^{32,33} and therefore allowing the direct interaction of the surface coating of the QDs (TOPO or fluorinated ligands) with the cellular membrane. In this way the impact of the presence of fluorine atoms on the QD surface could be truly investigated without being masked by adsorbed proteins.³⁴ As it can be seen in confocal images (Fig. 4), although both QDs types were efficiently internalized within cells, the extent of the cell uptake was significantly higher for QD_F. In order to quantify this uptake enhancement as a result of the presence of fluorinated ligands on the QD surface, the fluorescence density per cell was determined by analyzing the images with ImageJ (details in ESI). The fluorescence density within cells can be correlated to the amount of QDs internalized, and as shown in Fig. 3B,

QD_F were uptaken more efficiently by a factor of 5.7 in comparison with the control non-fluorinated QD_TOPO.

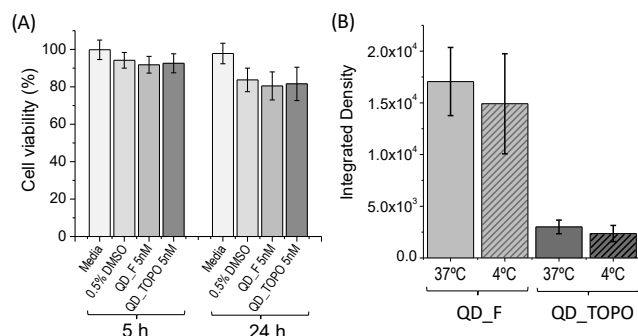


Figure 3. (A) Cell viability obtained by MTT assay of HeLa cells incubated for either 5 h or 24 h with QD_TOPO or QD_F (both at 5 nM). NPs were dispersed in serum-free cell medium containing 0.5% DMSO. (B) Quantification of fluorescence density per cell by analyzing confocal fluorescence images of HeLa cells incubated for 5 h with either QD_TOPO or QD_F (both at 5 nM) at 37 °C or 4 °C. For each case 50 cells were analyzed with ImageJ. Results are expressed as the mean \pm standard deviation (SD).

This enhanced cellular uptake of QD_F is consistent with the observed higher interaction with the cell membrane model, and allows concluding that increasing the surface activity of the QDs will lead to enhanced internalization by cells.

To further investigate if the uptake mechanism is via active or passive internalization processes, cells were incubated with QDs (QD_F and QD_TOPO 5 nM) at 4 °C, knowing that at this low temperature many cellular processes such as endocytosis of NPs are inhibited.³⁵ The amount of QDs internalized at 4 °C was only slightly lower than at 37 °C (Fig. 3B), which seems to indicate that these QDs can directly translocate through the lipid bilayer of the cell membrane by passive diffusion. This observation is in agreement with previous studies working with lipid-covered hydrophobic Au NPs of 5 nm, which demonstrated that hydrophobic NPs with diameters $d > 5$ nm translocate through the bilayer whereas individual NPs with diameters $d \leq 5$ nm are trapped in the bilayer. The only possibility of small hydrophobic NPs for leaving the bilayer is by forming clusters exceeding the threshold size.³⁶ Based on our previous work, we know that the QD_F are able to form nanoclusters in aqueous medium containing only a 5 % of DMSO,³⁷ and therefore our hypothesis is that these hydrophobic QDs, both QD_F and QD_TOPO, are crossing the cell membrane as clusters. The clear advantage of having clusters inside cells instead of single QDs is that the sensitivity towards bioimaging applications increases, because due to the more intense fluorescence of clusters the signal-to-noise ratio will be higher. Thus, it will allow to have a better discrimination from the fluorescence background (*i.e.* cell autofluorescence), which is a common issue that makes difficult to have an accurate and reliable diagnostic in cases where the sensitivity of the imaging probe is not good enough.

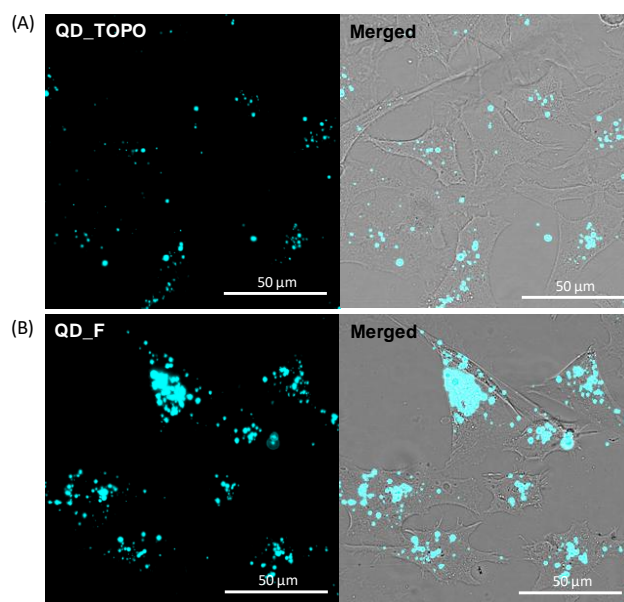


Figure 4. Confocal microscopy images of HeLa cells after incubation for 5 h at 37 °C with (A) QD_TOPO, or (B) QD_F (both at 5 nM). Incubation was performed in serum-free DMEM cell media containing 0.5 % of DMSO. Fluorescence channel was collected at 420-500 nm (λ_{ex} 405 nm). Single fluorescence channel and merged with the transmitted light channel are shown. The scale bar corresponds to 50 μ m.

In summary, fluorination of ZnCdS/ZnS QDs has successfully increased their interaction with a phospholipids interface, and consequently their surface activity. Such increase of surface activity is proposed as the key feature for the greater cellular internalization of the fluorinated QDs with respect to the non-fluorinated counterparts.

Extending our discussion beyond the data obtained for the NPs studied in the present work, the use of a DPPC phospholipid monolayer as a model for the cell membrane allows assessing differences in the surface activity of NPs. This points out the potential of such membrane model for establishing NP surface modification—surface activity relationships, which can be thereafter translated into surface activity—cell uptake correlations.

In the light of the presented findings it is suggested that fluorination of NPs can be exploited as a simple and universal strategy to promote NP—cell membrane interactions with the implication for their efficient cellular uptake. This work opens up new possibilities for the design of NP-based biomedical tools for diagnostic and therapy with improved uptake by cells, and consequently it may lead to improved performance.

Acknowledgements

Support from the MINECO is acknowledged through the following projects: CTQ2014-57515-C2 and CTQ2017-83961-R. J.J.G.-C. acknowledges MINECO for a Ramon y Cajal contract (RyC-2014-14956). CCC acknowledges MINECO for a Juan de la Cierva-Incorporación contract (IJCI-2014-19614). MC acknowledges Ikerbasque for a Research Associate Position.

Keywords: fluorination • quantum dots • Langmuir monolayer • surface activity • cell uptake

- [1] M. Björnmalm, K. J. Thurecht, M. Michael, A. M. Scott, and F. Caruso, *ACS Nano* **2017**, *11*, 9594.
- [2] E. Blanco, H. Shen, and M. Ferrari, *Nat. Biotechnol.*, **2015**, *33*, 941.
- [3] R. Thirupathi, S. Mishra, M. Ganapathy, P. Padmanabhan, and B. Gulyás, *Adv. Sci.* **2017**, *4*, 1600279.
- [4] S. Ahn, E. Seo, K. Kim, S. J. Lee, *Sci. Rep.* **2013**, *3*, 1997.
- [5] E. Polo, M. Collado, B. Pelaz, and P. del Pino, *ACS Nano* **2017**, *11*, 2397.
- [6] M. Reifarh, S. Hoepfner, and U. S. Schubert, *Adv. Mater.* **2018**, *30*, 1703704.
- [7] B. D. Chithrani, A. A. Ghazani, and W. C. Chan, *Nano Lett.* **2016**, *6*, 662.
- [8] M. Zhu, G. Nie, H. Meng, T. Xia, A. Nel, and Y. Zhao, *Acc. Chem. Res.* **2012**, *46*, 622.
- [9] E. C. Cho, L. Au, Q. Zhang, and Y. Xia, *Small* **2010**, *6*, 517.
- [10] S. Salatin, S. MalekiDizaj, and A. YariKhosroushahi, *Cell Biol. Int.* **2015**, *39*, 881.
- [11] Y. Jiang, S. Huo, T. Mizuhara, R. Das, Y. W. Lee, S. Hou, D. F. Moyano, B. Duncan, X. J. Liang, and V. M. Rotello, *ACS Nano* **2015**, *9*, 9986.
- [12] X. Xie, J. Liao, X. Shao, Q. Li, and Y. Lin, *Sci. Rep.* **2017**, *7*, 3827.
- [13] K. Saha, D. F. Moyano, and V. M. Rotello, *Mater. Horiz.* **2014**, *1*, 102.
- [14] Y. Li, X. Chen, and N. Gu, *J. Phys. Chem. B* **2008**, *112*, 16647.
- [15] L. Liu, J. Zhang, X. Zhao, Z. Mao, N. Liu, Y. Zhanga, Q. H. Liu, *Phys. Chem. Chem. Phys.* **2016**, *18*, 31946.
- [16] M. SamadiMoghaddam, M. Heiny, and V. P. Shastri, *Chem. Commun.* **2015**, *51*, 14605.
- [17] Y. L. Chiu, Y. C. Ho, Y. M. Chen, S. F. Peng, C. J. Ke, K. J. Chen, F. L. Mi, and H. W. Sung, *J. Control. Release* **2010**, *146*, 152.
- [18] E. P. Gillis, K. J. Eastman, M. D. Hill, D. J. Donnelly, and N. A. Meanwell, *J. Med. Chem.* **2015**, *58*, 8315.
- [19] J. Wang, M. Sánchez-Roselló, J. L. Aceña, C. del Pozo, A. E. Sorochinsky, S. Fustero, V. A. Soloshonok, and H. Liu, *Chem. Rev.* **2013**, *114*, 2432.
- [20] T. Fischer, and R. Riedl, *ChemistryOpen* **2017**, *6*, 192.
- [21] M. Boccalon, P. Franchi, M. Lucarini, J. J. Delgado, F. Sousa, F. Stellacci, I. Zucca, A. Scotti, R. Spreafico, P. Pengo, and L. Pasquato, *Chem. Commun.* **2013**, *49*, 8794.
- [22] P. Zrazhevskiy, M. Sena, and X. Gao, *Chem. Soc. Rev.* **2010**, *39*, 4326.
- [23] K. D. Wegner, and N. Hildebrandt, *Chem. Soc. Rev.* **2015**, *44*, 4792.
- [24] X. Yang, K. Zhanghao, H. Wang, Y. Liu, F. Wang, X. Zhang, K. Shi, J. Gao, D. Jin, and P. Xi, *ACS Photonics* **2016**, *3*, 1611.
- [25] C. Carrillo-Carrión, M. Gallego, W. J. Parak, and M. Carril, *Materials* **2018**, *9*, 750.
- [26] A. T. R. Williams, S. A. Winfield, and J. N. Miller, *Analyst*, **1983**, *108*, 1067.
- [27] W. J. M. Lokerse, E. C. M. Kneepkens, T. L. M. ten Hagen, A. M. M. Eggemont, H. Grull and G. A. Koning, *Biomaterials* **2016**, *82*, 138.
- [28] J. Gao, R. S. Ndong, M. B. Shiflett and N. J. Wagner, *ACS Nano* **2015**, *9*, 3243.
- [29] J. J. Giner-Casares, G. Brezesinski and H. Möhwald, *Curr. Opin. Colloid Interface Sci.* **2014**, *19*, 176.
- [30] J. P. Coelho, M. J. Mayoral, L. Camacho, M. T. Martín-Romero, G. Tardajos, I. López-Montero, E. Sanz, D. Ávila-Brandé, J. J. Giner-Casares, G. Fernández and A. Guerrero-Martínez, *J. Am. Chem. Soc.* **2017**, *139*, 1120.
- [31] J. J. Giner-Casares, and J. Reguera, *Nanoscale* **2016**, *8*, 16589.
- [32] I. Lynch, K. A. Dawson, *Nano Today* **2008**, *3*, 40.
- [33] C. D. Walkey, W. C. W. Chan, *Chem. Soc. Rev.* **2012**, *41*, 2780.
- [34] A. Salvati, A. S. Pitek, M. P. Monopoli, K. Prapainop, F. BaldelliBombelli, D. R. Hristov, P. M. Kelly, C. Åberg, E. Mahon, K. A. Dawson, *Nat. Nanotechnol.* **2013**, *8*, 137.
- [35] T. Dos Santos, J. Varela, I. Lynch, A. Salvati, K. A. Dawson, *PloSone*, **2011**, *6*, e24438.
- [36] Y. Guo, E. Terazzi, R. Seemann, J. B. Fleury, and V. A. Baulin, *Sci. Adv.*, **2016**, *2*, e1600261.
- [37] C. Carrillo-Carrión, M. Atabakhshi-Kashi, M. Carril, K. Khajeh, and W. J. Parak, *Angew. Chem. Int. Ed.*, **2018**, *57*, 5033.

Entry for the Table of Contents (Please choose one layout)

Layout 1:

COMMUNICATION

Text for Table of Contents

Fluorination of NPs is presented as strategy to promote NP–cell membrane interactions with the implication for their efficient cellular uptake. The increased surface activity of the fluorinated NPs, which is demonstrated by using Langmuir monolayers as cell model membrane, seems to be the key feature for their enhanced cell uptake.



Author(s), Corresponding Author(s)*

Page No. – Page No.

Title